

Assessment of *Miscanthus x giganteus* derived biochar as copper and zinc adsorbent: study of the effect of pyrolysis temperature, pH and hydrogen peroxide modification

DOI: 10.1016/j.jclepro.2017.06.114

Alessio Cibati^{a,d*}, Bente Foereid^{b,d}, Ajay Bissessur^a, Simona Hapca^d

^aSchool of Engineering, University of KwaZulu-Natal, Howard College Campus, Durban, South Africa ^bNIBIO, Norwegian Institute of Bioeconomy Research, Norway

^aSchool of Chemistry and Physics, University of KwaZulu-Natal, Howard College Campus, Durban, South Africa ^dSIMBIOS Centre, Abertay University of Dundee, Bell Street, Dundee (Scotland, UK) *Corresponding author: e-mail: cibale1983@gmail.com

Abstract

In this work, experimental and modelling investigations were conducted on biochars pyrolyzed at 350°C and 600°C, to determine the effect of pyrolysis temperature, hydrogen peroxide activation and pH on copper and zinc removal, in comparison with commercially available activated carbons. Characterization of biochars was performed by BET surface area, elemental analysis and FTIR spectroscopy. Experiments results demonstrated that biochar pyrolyzed at 600°C adsorbed both copper and zinc more efficiently than biochar pyrolyzed at 350°C. Chemical activation by H₂O₂ increased the removal capacity of biochar pyrolyzed at 350°C. All investigated biochars showed a stronger affinity for copper retention, with a maximum adsorption capacity of 15.7 mg/g while zinc was 10.4 mg/g. The best adsorption performances were obtained at pH 5 and 6. Langmuir adsorption isotherm described copper adsorption process satisfactorily, while zinc adsorption was better described by Freundlich isotherm.

Keywords: Biochar; metal adsorption; isotherms; adsorbent; copper; zinc

1. Introduction

Environmental contamination by metals has become a serious problem due to their indefinite persistence in the environment which lead to water, air and soil contamination and health risks. Metals can be released into the environment from several industrial processes such as mining, metal processing, automobile manufacturing, refining of ores and combustion of fossil fuels (Tchounwou et al., 2012; Margui et al., 2004). Copper and zinc are widely used for many purposes like electrical appliances, electronics, automotive, paint and battery, as well as compounds in fungicides, algicides, insecticides, fertilisers and pesticides. Given their toxic effect, their discharge into the environment can pose risk for human health. The limits in drinking water are 1 mg/L and 5 mg/L for copper and zinc, (Secondary Maximum Contaminant Level) (EPA, 2016).

In the past years, methods such as Fenton- chemical precipitation (Fu et al., 2012), ionexchange (Dabrowski et al., 2004), , membrane filtration (Malamis et al., 2011), electrocoagulation (Akbal and Camci, 2011) and adsorption (Boudrahem et al., 2011; F Turan et al., 2011) among the others, have been optimized to regenerate waters and industrial wastewaters contaminated by heavy metals.

Boudrahem et al. (2011), studied modified activated carbons derived from coffee residue through a chemical activation using zinc chloride and phosphoric acid, which led to a modification of the pore structure and enhanced the adsorption capacity of the adsorbent. Similarly, Trevino-Cordero et al. (2013), proved the suitability of fruits plant derived activated carbons for the removal of contaminants in water and showed the positive effects of impregnation with calcium salts on the surface of the activated carbons. Currently, adsorption has been proved as one of the most promising techniques and activated carbon (AC) is currently one of the most used adsorbents in such treatments. However, the necessity to find more

cost-effective treatments have led researchers to explore the feasibility of low-cost materials as metals adsorbent. Materials like zero valent iron, agricultural waste such as nut shell, fruit bagasse, rice and coconut husk, egg shells, seafood waste and chitosan have been investigated as material for the removal of metals and other pollutants from water (Lim and Aris, 2013). Other researchers have investigated the production and use of biochar from feedstocks such as plant residues (Chen et al., 2011; Yao et al., 2011), animal manures (Cao and Harris, 2010), sewage sludge (Wang et al., 2011) and swine manure (Meng et al., 2014)

Biochar is a carbon rich material produced by combustion under reduced oxygen supply (pyrolysis) of organic (plant, wood, agricultural waste, sludge, poultry litter) materials.

Miscanthus x giganteus is a plant grown in Europe and widely studied as energy crops (Lewandowski et al., 2000; Brosse et al., 2012), crop for co-firing with coal to produce power and reduce CO₂ emission (Heaton et al., 2004; Clifton-Brown et al., 2007), feedstock for second generation biofuels (; Melligan et al., 2012) and as soil amendment (; Kwapinski et al., 2010; Houben et al., 2014). Despite *Miscanthus x giganteus* derived biochar has been proved as a suitable soil amendment, and has shown good physical/chemical properties for metals uptake (Mimmo et al., 2014), no studies have been conducted so far to test the capacities of *Miscanthus x giganteus* derived biochar to adsorb metals from aqueous solutions. Mimmo et al. (2014), pointed out the effect of pyrolysis temperature on biochar structure showing physical/chemical changes of surface and porous structure, indicating 360°C as threshold above which aromatic structures increase and O/C and H/C ratios decrease.

In this framework, this study investigated the capacities of a biochar derived from *Miscanthus x giganteus* plant as copper and zinc adsorbent. Being adsorption influenced by many factors including pH, pyrolysis temperature, and presence of oxygen-containing functional groups on adsorbent's surface, a comprehensive investigation on *Miscanthus x giganteus* derived biochar

under different operating conditions was conducted along with modelling studies through equilibrium isotherm equations. Moreover, two types of activated carbons (AC Fluval and AC Norit) were tested for comparison. *Miscanthus x giganteus* raw biomass, due to its low performance was included in the study as a control.

2. Materials and Methods

2.1 *Miscanthus x giganteus* biochar

Feedstock for the biochar used in this study *Miscanthus x giganteus*, a perennial warm-season (C4) grass, was sourced from Adare, Limerick, Ireland. Biochar was produced by pyrolysis in a furnace at 250 atm at two different temperature, 350°C and 600°C (BC350 and BC600, respectively) for 10 min using nitrogen gas to prevent complete combustion; then it was cooled for 10 min in a tube under a nitrogen rich atmosphere.

2.2 Activated carbon

Two types of commercially available activated carbon (AC norit and AC fluval) were used in this study. AC norit, a granular activated carbon produced by steam activation of coal, has an average diameter of 1 mm, is suitable for potable water processing and industrial process liquids. Fluval carbon, a pure activated carbon is used in both fresh and salt water treatments. The inner matrix structure provides a large porous area that permanently traps organic and inorganic wastes and removes many other impurities from the water.

2.3 Chemical and physical characterisation of biochars

The specific surface areas (SA) were measured with N₂ (g) adsorption at 77 K determined by a Tristar II3020 surface area analyzer (Micromeritics Instrument Co., USA). Specific surface

areas (SBET) were taken from adsorption isotherms using the Brunauer, Emmett and Teller (BET) equation (Brunauer et al., 1938). Elemental analysis of carbon (C), hydrogen (H), oxygen (O) and nitrogen (N) was conducted by ThermoScientific Flash 2000 organic elemental analyser. FT-IR analysis was conducted using a Perkin Elmer Spectrum RX1 FT-IR spectrometer to establish the nature of the biochar and the changes to the structure as a consequence of both pyrolysis and chemical activation.

2.4 Adsorption batch experiments

Batch experiments were performed to investigate the adsorption capacity of biochar and activated carbon on copper and zinc metal ions from aqueous solutions. In each experiment, an aliquot mass of 1 g of adsorbent was mixed with 50 mL of Cu^{2+} (aq) and Zn^{2+} (aq) solutions at different initial concentrations (mg/L): 63.5; 158.5; 317.7; 635.4; 1,270.8 for copper solutions, and 65.3; 163.4; 327; 653.8; 1,307.6 (mg/L) for zinc solutions in a 250 mL Erlenmeyer flask. The Cu^{2+} (aq) and Zn^{2+} (aq) ions were introduced in the synthetic solutions as copper sulfate ($\text{CuSO}_4 \cdot 5\text{H}_2\text{O}$) and zinc sulfate ($\text{ZnSO}_4 \cdot 7\text{H}_2\text{O}$). All chemicals used were of analytical grade supplied by Sigma Aldrich. Solutions were prepared with ultrapure water produced by Milli-Q gradient unit (Millipore). Initial tests showed that the amount removed had stabilised after 1 hour (h), for this reason each experiment was carried out for 1 h. The mixture was agitated at 120 rpm on a shaker at room temperature and samples were taken at intervals of 15 min. The samples then were immediately filtered with 0.45 μm Whatman filter and the filtrates were analysed for residual metals concentrations in solution by Atomic Absorption Spectroscopy (AAAnalysist 200 Perkin Elmer Inc, Shelton CT, USA). All batch experiments conducted in this work were conducted in a duplicate way.

2.4.1 Operative conditions

Different sets of experiments were carried on in order to optimize the adsorption process by investigating the effect of pyrolysis temperature, pH value, modification by H₂O₂.

2.4.1.1 Pyrolysis temperature

1
2
3
4
5
6
7
8
9
10
11
12
13
14
15
16
17
18
19
20
21
22

The effect of the pyrolysis temperature on the adsorption capacity of biochar was investigated by comparing samples BC350, BC600 and raw *Mischantus x giganteus*. Batch tests were conducted as described above.

2.4.1.2 Chemical activation by H₂O₂

Biochars, BC350 and BC600, were both pyrolyzed at 350 and 600°C and chemically activated using H₂O₂ as follows: A 3.0 g mass aliquot of BC was added to 40 ml of H₂O₂(aq) solution (10 % w/v) for 2hrs with continuous agitation at room temperature. After rinsing with deionized water and drying at 80°C, the resulting activated BC350 and BC600 (BC350 ACT and

BC600 ACT) were stored in a sealed plastic container in a cold room at 4°C for later experiments. The adsorption capacity of BC350 ACT and BC600 ACT was investigated in batch experiments and compared to BC350, BC600, AC norit and AC fluval.

2.4.1.3 pH value

The effect of pH was studied by settling experiments at pH 4, 5 and 6. The pH during the experiment was constantly monitored and kept constant by adding drops of NaOH and HCl (0.1 M). All batch experiments were conducted as described above in the section 2.4.

2.5 Model formulation and statistical analysis

Pseudo-first-order (Eq. 1) and pseudo-second-order (Eq. 2) models were used to simulate the sorption kinetics data (Lagergren, 1898; Ho and McKay, 1999):

$$\log(q_{ee} - q_{qt}) = \log q_{ee} - \frac{K}{2.303} t \quad (1)$$

$$\frac{q_t}{q_{te}} = \frac{K_2 t}{1 + K_2 t} + \frac{1}{1 + K_2 t} \quad (2)$$

1
2
3
4
23
24
25
6
7
8
9
11
12
13
14
15

where q_{tt} and q_{ee} (mg/g) are adsorbed copper and zinc amount at time t (h) and equilibrium, KK_1 (1/h) and KK_2 (g/(mg h)) are the rate constant for the pseudo-first-order and pseudo-second-order adsorption kinetics, respectively. The linear plots of value $\log(q_{ee} - q_{tt})$ against time, can give the pseudo-first-order adsorption rate constant KK_1 from the slope and q_{ee} can be calculated from the intercept. By plotting t/q_{tt} against time t , the pseudo-second-order adsorption rate constant KK_2 and q_{ee} were determined from the intercept and slope of the plot. The corresponding values of KK_1 , q_{ee} and R^2 are presented in Table 3 at tested metals concentrations. Adsorption models 5 based on Langmuir and Freundlich equations were fitted to the data. The Langmuir model assumes monolayer adsorption onto a homogeneous surface with no interactions between the adsorbed molecules. The Freundlich model is an empirical equation commonly used for heterogeneous surfaces in the low to intermediate concentration range adsorption system (Gerente et al., 2007;). The concentration of Cu^{2+} (aq) and Zn^{2+} (aq) sorbed onto BC was 10 calculated according to the following equation ():

$$Q_{ee} = \frac{V}{V_0} \frac{C_0 - C_{ee}}{C_{ee}} \quad (3)$$

where Q_e (mg/g) is the amount of Cu^{2+} (aq) or Zn^{2+} (aq) adsorbed at equilibrium. C_0 and C_e (mg/L) are the initial and equilibrium Cu^{2+} (aq) or Zn^{2+} (aq) concentration in solution. g (gram) is the mass of BC. The experimental data were fitted by Langmuir and Freundlich isotherms according to the following equations:

1
2
3
4
16
17
18
19
20
21
22
23
24
5
6
7
8
9

Langmuir: $Q_e = \frac{K Q_{max} C_e}{1 + K C_e}$
(4)

Where Q_e is the amount of metal adsorbed per unit weight of adsorbent (mg/g), C_e is the equilibrium concentration of solute bulk solution (mg/L), Q_{max} is the maximum monolayer adsorption capacity (mg/g) and k is the constant related to free energy.

Freundlich $Q_e = K_f C_e^{1/n}$ (5)

Where Q_e is the amount of solute adsorbed per unit weight of adsorbent (mg/g), C_e is the equilibrium concentration of solute in solution (mg/L), K_f is the relative adsorption capacity constant of the adsorbent (mg/g) and n is the Freundlich linearity constant and it is indicative of bond energies between metal ion and the adsorbent. The Freundlich constants can be obtained from the plot of $\ln Q_e$ against $\ln C_e$. Statistical analysis was performed in R Statistical Package v.2.12,[□] and comparison of the two models' performance was conducted based on the AIC model selection criterion (Fox, 2008) as provided in R. It was determined if the coefficients in the equation were different from 0 and treatments were compared pairwise to determine if the coefficients for the equations for different treatments were different from each other. Separate pairwise comparisons were carried out between types of biochar or activated carbon within each pH level, and between pH levels within each biochar/activated carbon. Furthermore, a study of the adsorption selectivity of copper and zinc by the biochars was

conducted by analyzing the distribution coefficient (K_d cm³/g). K_d is an indicator used for the selectivity of the adsorbent to the particular ion in the presence of other ions (Lin et al., 2001):

1

2

3

4

$$K_d = \frac{C_0 - C_f}{C_f} \cdot \frac{V}{g} \quad (6)$$

12 where C_0 and C_f (mg/cm^3) are the initial and equilibrium concentrations of a metal species,
 13 respectively. V (cm^3) is the volume of the solution, and g (gram) is the amount of
 adsorbent. A

14 selectivity coefficient (α), (dimensionless), for the binding of a specific metal ion in the 15
 presence of others is given by (Kang et al., 2004):

$$\alpha = \frac{K_d(T)}{K_d(I)} \quad (7)$$

17 where $K_d(T)$ is the K_d value of the targeted metal ($\text{Cu}^{2+}(\text{aq})$ ions in this case), and $K_d(I)$ is the
 18 K_d value of zinc. The greater the value of α , the better the selectivity toward copper over
 zinc.

19

20 **3. Results and discussion 21 3.1 Biochar characterization**

22 The physico-chemical characteristics of biochars (both activated and non-activated) used in
 23 this study are shown in Table 1. BET analysis showed that the pyrolysis temperature do not
 24 remarkably affect the surface area, while the pore size of BC600 was about twice the size of
 25 BC350. Chemical activation of biochar pyrolyzed at lower temperature (BC350 ACT) showed

1 a significant increase in BET surface area from 0.71 to 6.50 m²/g relative to inactivated biochar
 2 (BC350) (Table 1). However, a small increase from 0.72 to 0.95 m²/g was observed for
 3 chemical activation of biochar (BC600 ACT) relative to the inactivated biochar (BC600)
 4 (Table 1). The negligible increase in surface area for biochar pyrolyzed at higher temperature
 5 could be due to the increase of volatile fractions which reduce the pores availability (Wang et
 6 al., 2016). Chemical activation also increased the micropore volume for both biochars, while
 7 had a negligible effect on the pore size for biochar pyrolyzed at lower temperature and
 8 detrimental effect on biochar pyrolyzed at 600°C. The pH of the biochar samples treated with
 9 H₂O₂ was lower respect to the natural counterpart, which can be attributed to the presence of
 10 carboxyl surface functional groups, as observed by other authors (Huff and Lee, 2016; Xue et
 11 al., 2012). In addition, Huff and Lee (2016) also showed a higher cation exchange capacity
 12 (CEC) after H₂O₂ activation due to the addition of acidic oxygen functional groups on the
 13 surface of the biochar.

14 **Table 1.** Physiochemical properties of biochars.

Adsorbent	pH -	BET surface area (m²/g)	t-PLOT Micropore volume (cm³/g)	Pore size (nm)
BC350	8.30	0.71	0.000701	5.78
BC600	5.97	0.72	0.000334	11.48
BC350 ACT	5.82	6.50	0.0024	6.43
BC600 ACT	5.40	0.95	0.0014	5.40

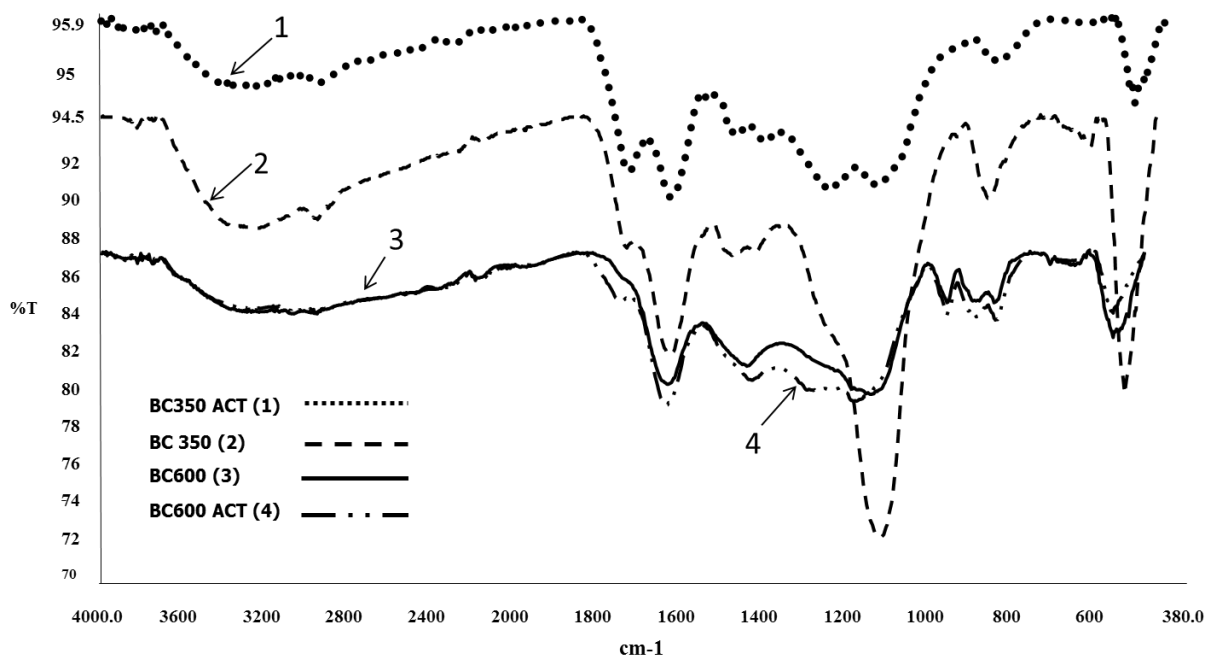
15
 16 Elemental analyses as well as O/C and H/C ratios are helpful indicators to provide biochars'
 17 characterization. Results (Table 2) indicate that an increase of pyrolysis temperature reflected
 18 a higher loss of oxygen and hydrogen content, while the carbon content increased. As a
 19 consequence of dehydration and decarboxylation reactions which occur at higher temperature,
 20 BC600 showed a decreased O/C and H/C ratios, leading to a more stable aromatic-like
 21 structure. On the other hand, chemical activation had a noticeable effect on the oxygen content

of BC350, resulting in the highest O/C ratio, highest oxygen percentage and lowest carbon 1
percentage for the substrate, due to an increase of the oxygen-containing groups and negative
2 charges(Table 2), as also observed by others (Wang et al., 2016).

Table 2. Elemental analysis of biochars.

Adsorbent	N (%)	C (%)	H (%)	O (%)	O/C	H/C
BC350	0.77	64.48	3.85	14.82	0.22	0.05
BC600	0.30	73.99	2.23	6.91	0.09	0.03
BC350 ACT	1.07	62.4	3.74	20.19	0.32	0.05
BC600 ACT	0.38	77.79	2.40	6.01	0.07	0.03

The Fourier transform infrared spectroscopy (Figure 1) was used as an effective qualitative tool
in investigating functional group changes during the pyrolysis of biochars. For pyrolyzed
biochar the important stretching vibrations are the O-H at 3400 cm^{-1} , the aliphatic C-H stretch
between 3000-2860 cm^{-1} , the aromatic C-H stretch at 3060 cm^{-1} , the carboxyl (C=O) stretch at
1700 cm^{-1} , aromatic ring stretching modes at 1590 and 1515 cm^{-1} , the C-O-(C) stretch at 1275
 cm^{-1} and the C-O-(H) stretch at approx. 1050 cm^{-1} . According to Sun and Tomkinson, (2001)
and Bouwman and Freriks (1980), the spectral band at 1600 cm^{-1} can be due to the aromatic
skeletal mode. BC350 and BC350 ACT spectra are similar to each other but more intense than
the BC600 and BC600 ACT spectra. Both BC350 and BC 350ACT are dominated by stretching
frequencies of the OH at between 3400 cm^{-1} to 3600 cm^{-1} , the C-H stretching between 3000
 cm^{-1} and 2800 cm^{-1} , aromatic skeletal mode at approx. 1600 cm^{-1} and the C-O-(H) stretch at
approx. 1050 cm^{-1} .



39

40 **Figure 1.** FT-IR analysis of all biochars investigated.

41 The BC350 sample showed much larger absorption energies than the BC350ACT samples due
 42 to O-H bond stretching at around 3300cm⁻¹, C-O⁺=C or C=O stretches at 1600 cm⁻¹ and C-O
 43 stretch at around 1100 cm⁻¹ than the BC350ACT samples.

44 Moreover, a decreased intensity related to an increased transmittance was observed for bands
 45 associated with aromatic groups (1580-1600 and 3050-3000 cm⁻¹). These results are in
 46 accordance with previous studies (Al-Wabel et al., 2013; Yuan et al., 2011; Novak et al., 2009),
 47 which have shown that the presence of functional groups are associated with biochar pyrolyzed
 48 at lower temperature (300-500°C) and are absent or negligible at higher temperature
 49 (500-700°C). These data are in accordance with those of the atomic ratios (Table 2) which
 50 indicated a decrease of oxygen group and an increase of C-structure, leading to a decrease of
 51 biochar's polarity and to an increase of the aromatic structure at higher temperature. Similarly,
 52 Huff and Lee (2016), observed changes between treated and untreated samples occurred at
 53 1585 cm⁻¹ (C=C stretching), indicating that the H₂O₂ treatment caused an alteration of the
 54 aromatic carbon content. Conversely, the H₂O₂ treatment caused an increase of the peaks (1315

55 and 1700 cm^{-1}) correlated with the carboxylic functionality (Fig.1) as also observed by Huff
56 and Lee (2016). In the finger printing region (1100-500 cm^{-1}), higher temperature induced an
57 aromatic C-H deformation (850-800 cm^{-1}). Similar vibrations in the fingerprint region of
58 *Mischantus x giganteus* biochar pyrolyzed at different temperature were also observed by
59 Mimmo et al. (2014). In this region, also the H_2O_2 treatment led to an increase in C-H stretching
60 probably due to conversion from aromatic C=C ring structure (Wang and Griffiths, 1985; Huff
61 and Lee, 2016). Biochar pyrolyzed at 600°C showed less intense infrared peaks due to an
62 increase in the carbon activity and with progression of the pyrolysis at 600°C there is evident
63 disappearance of O-H and C-H stretches mainly due to dehydration. It is possible at this stage
64 that the C-H peaks move from aliphatic to becoming aromatic C-H peaks and then disappear
65 as suggested by Cheng, et al. (2008). The BC 600 and BC 600 ACT spectra are similar and are
66 dominated by the stretching aromatic skeletal mode at 1600 cm^{-1} and the C-O-(H) stretch at
67 1050 cm^{-1} .

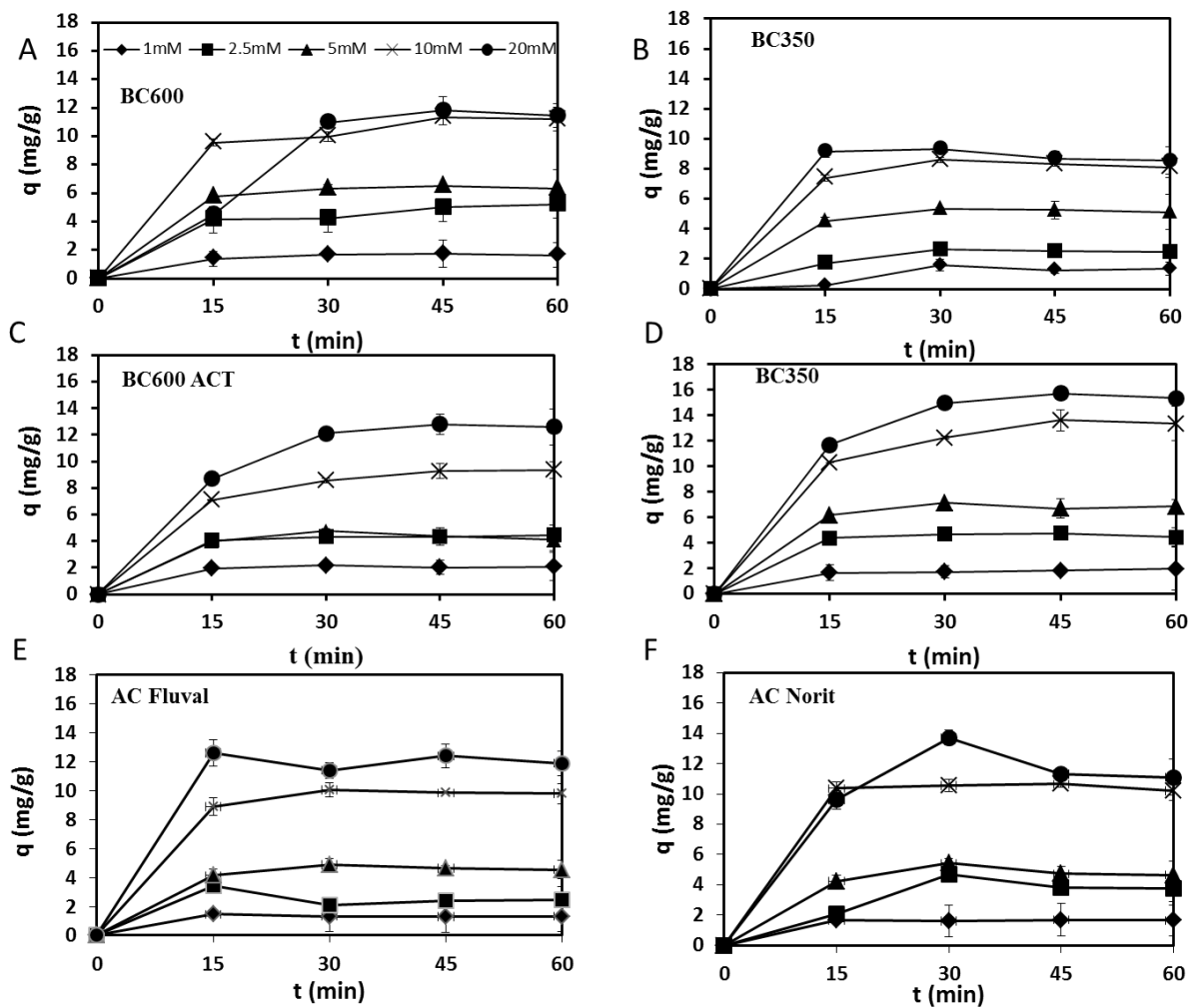
68

69 **3.2 Batch experiments results**

70 **3.2.1 Adsorption kinetics**

71 The effect of the contact time on the adsorption of copper and zinc (at pH 6) was studied (Fig.
72 2 and 3, respectively). Pseudo-first-order and pseudo-second-order models were applied to
73 describe the copper and zinc kinetics removal and the obtained kinetics parameters were
74 reported in Table 3.

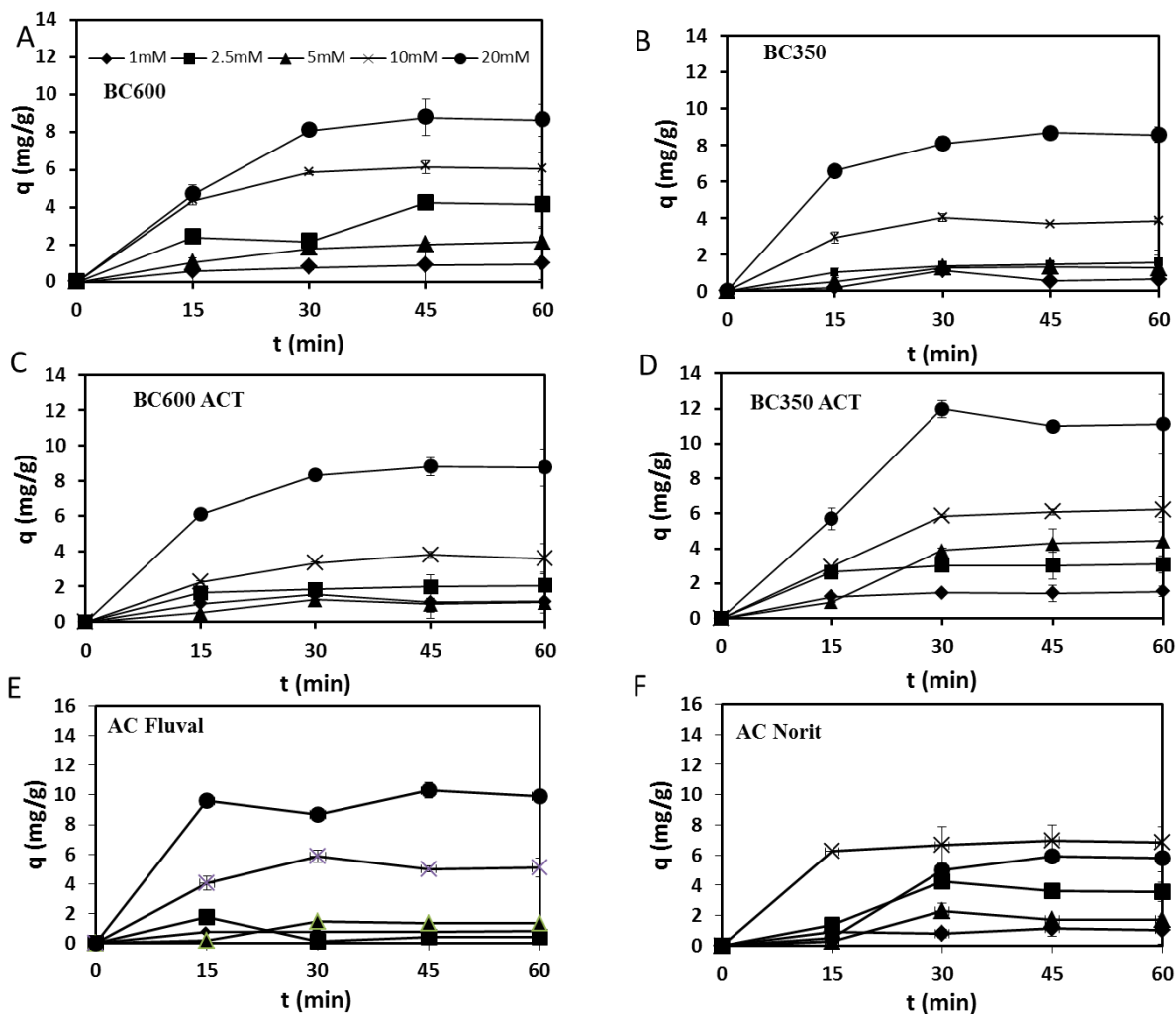
75



1

2 **Figure 2.** Effect of contact time on copper adsorption capacities at pH 6 for BC600 (A),
 3 BC350 (B), BC600ACT (C), BC350ACT (D), AC Fluval (E) and AC Norit (F).

4



1
 2 **Figure 3.** Effect of contact time on zinc adsorption capacities at pH 6 for BC600 (A), BC350
 3 (B), BC600ACT (C), BC350ACT (D), AC Fluval (E) and AC Norit (F).
 4

5 Metals adsorption was fast, with more than 60-70 % of adsorption occurring within 15 min,
 6 while after 30 min more than 90% of the total adsorption occurred. Similar results were also
 7 observed from Mohan et al. (2007), with 40–70% of the total metal adsorption occurred within
 8 the 60 min. Similarly to others (Moreira and Alleoni, 2010), the amount of adsorbed metal
 9 increased as the initial concentration increased (Fig. 2 and 3), as well as the competition among
 10 the metals for the adsorption sites. As matter of result, copper was preferentially adsorbed than
 11 zinc onto the four different substrates. The higher affinity of copper over zinc and other metals
 12 was also observed for other organic matrices by Fontes and Gomes (2003). Fontes et al. (2000),
 13 pointed out that zinc is more influenced by electrostatic interactions with the active sites of the

14 surface, whereas copper is more affected by covalent binding, and this is given by the higher
15 ionic potential (ratio between the charge and radius of an ion) of copper (5.48) respect to zinc
16 (5.33), confirming a greater ability of copper to bind through electrostatic interactions. Despite
17 related works (Xue et al., 2012), showed a faster adsorption after the modification by hydrogen
18 peroxide of peanut biochar, in this case, the modification of biochar by hydrogen peroxide did
19 not increase the adsorption rate, but an increased amount of metal removal was observed for
20 modified biochars pyrolyzed at lower temperature (Fig. 2D, 3D and Fig. 5). As showed in
21 Table 2, the enhanced adsorption capacity of oxidized biochar produced at lower temperature
22 is explained by the increase of O/C ratios, a greater drop of pH and by an increase of negative
23 charges on the biochar surface who lead to a higher attraction of positive charged metal cations
24 . Experimental results were fitted by pseudo-first-order and pseudo-second-order kinetic
25 models to better describe the heavy metal adsorption mechanism. The values KK_1 and KK_2 ,
26 calculated qq_{ee} values and the correlation coefficients R^2 are reported in Table 3.

27 **Table 3.** Parameters of pseudo-first-order and pseudo-second-order kinetics models for copper
28 and zinc adsorption onto BC600 ACT, BC350 ACT, BC600 and BC350.

29

Adsorbent	Metal	pH	Initial	Pseudo-first-order			Pseudo-second-order			Metal	pH	Initial	Pseudo-first-order			Pseudo-second-order		
			Conc. Cu	K ₁	Q _e	R ²	K ₂	Q _e	R ²			Conc. Zn	K ₁	Q _e	R ²	K ₂	Q _e	R ²
BC600 ACT	Cu	6	63.5	0.018	0.66	0.34	2.56	2.08	0.99	Zn	6	65.3	0.0073	0.79	0.15	0.95	1.15	0.97
			158.5	0.0028	1.11	0.88	0.28	4.55	0.99			163.4	0.021	1.51	0.94	0.22	2.08	0.99
			317.7	0.0076	3.31	0.22	0.31	4.35	0.99			327	0.012	0.47	0.42	0.11	1.22	0.87
			635.4	0.012	3.80	0.98	0.04	10.00	0.99			653.8	0.022	3.02	0.75	0.06	4.00	0.96
			1,270.8	0.0039	1.11	0.82	0.02	14.29	0.98			1,307.6	0.03	7.24	0.90	0.03	10.00	0.98
	Cu	5	63.5	0.009	0.51	0.25	1.25	1.22	0.99	Zn	5	65.3	0.001	0.15	0.003	1.56	0.31	0.95
			158.5	0.022	1.29	0.88	0.33	2.13	0.99			163.4	0.019	1.08	0.95	0.13	1.14	0.94
			317.7	0.025	2.69	0.91	0.13	3.70	0.99			327	0.023	1.55	0.95	0.15	1.85	0.98
			635.4	0.022	4.17	0.75	0.02	4.55	0.86			653.8	0.034	5.25	0.89	0.06	6.67	0.99
			1,270.8	0.013	2.82	0.92	0.08	3.23	0.97			1,307.6	0.003	4.68	0.12	0.03	5.56	0.92
	Cu	4	63.5	0.005	0.28	0.49	2.81	0.08	0.89	Zn	4	65.3	0.006	0.19	0.85	0.67	0.13	0.80
			158.5	1.E-05	1.26	0.0001	1.01	0.09	0.98			163.4	0.009	0.54	0.73	2.35	0.18	0.89
			317.7	0.022	1.82	0.78	0.12	2.78	0.98			327	0.014	2.45	0.92	0.21	2.63	0.98
			635.4	0.0002	1.78	0.001	0.25	0.89	0.99			653.8	0.0012	2.09	0.002	0.03	2.94	0.76
			1,270.8	0.0321	8.32	0.98	0.009	7.69	0.85			1,307.6	0.004	0.86	0.03	0.05	14.29	0.99
BC350 ACT	Cu	6	63.5	0.018	1.32	0.88	0.28	1.96	0.99	Zn	6	65.3	0.017	1.06	0.84	0.35	1.56	0.99
			158.5	0.027	2.51	0.88	1.21	4.55	0.99			163.4	0.021	1.74	0.83	0.28	3.13	0.99
			317.7	0.0008	1.78	0.03	0.33	7.14	0.99			327	0.024	5.37	0.95	0.004	7.14	0.93
			635.4	0.029	10.23	0.83	0.03	14.29	0.99			653.8	0.033	6.92	0.97	0.02	7.14	0.90
			1,270.8	0.031	10.23	0.74	0.03	16.67	0.99			1,307.6	0.0048	1.20	0.03	0.01	12.5	0.92
	Cu	5	63.5	0.006	0.66	0.19	0.89	1.23	0.99	Zn	5	65.3	0.0018	0.13	0.01	3.88	0.81	0.98
			158.5	0.022	1.51	0.78	0.43	3.13	0.99			163.4	0.021	2.34	0.97	0.05	2.17	0.90
			317.7	0.024	3.39	0.94	0.10	5	0.99			327	0.0015	1.32	0.14	0.10	2.38	0.97
			635.4	0.023	6.46	0.96	0.05	8.3	0.99			653.8	0.028	5.37	0.91	0.10	8.33	0.99
			1,270.8	0.034	12.30	0.95	0.0001	33.3	0.93			1,307.6	0.023	0.13	0.69	0.01	11.11	0.86
	Cu	4	63.5	0.016	0.66	0.98	0.24	0.67	0.95	Zn	4	65.3	0.015	0.49	0.95	0.37	0.5	0.95
			158.5	0.016	0.95	0.89	2.28	1.13	0.99			163.4	0.012	0.87	0.93	0.05	0.77	0.90
			317.7	0.023	2.82	0.81	0.08	3.75	0.98			327	0.013	2.88	0.89	0.07	3.33	0.97
			635.4	0.034	5.13	0.89	0.001	11.11	0.96			653.8	0.022	3.98	0.99	0.03	3.85	0.90
			1,270.8	0.028	7.94	0.91	0.03	6.96	0.93			1,307.6	0.018	3.16	0.96	0.02	2.86	0.79
BC600	Cu	6	63.5	0.017	1.04	0.71	0.50	1.71	0.99	Zn	6	65.3	0.015	0.99	0.98	0.17	1.03	0.96
			158.5	0.028	4.79	0.95	0.06	5.31	0.98			163.4	0.027	5.13	0.77	0.02	4.55	0.92
			317.7	0.024	2.82	0.71	0.25	6.46	0.99			327	0.022	2.34	0.99	0.05	2.38	0.92
			635.4	0.03	7.94	0.81	0.04	11.44	0.99			653.8	0.028	4.37	0.84	0.05	6.25	0.98
			1,270.8	0.034	11.48	0.69	0.01	12.99	0.89			1,307.6	0.034	8.51	0.79	0.02	9.09	0.94
	Cu	5	63.5	0.018	0.59	0.84	0.47	0.81	0.98	Zn	5	65.3	0.009	0.47	0.51	0.12	0.5	0.90
			158.5	0.014	0.92	0.56	0.50	1.47	0.99			163.4	0.02	1.38	0.98	0.07	1.37	0.88
			317.7	0.01	2.40	0.64	0.48	3.23	0.99			327	0.001	2.88	0.57	0.05	2.86	0.93
			635.4	0.025	4.79	0.86	0.06	6.67	0.98			653.8	0.027	6.46	0.78	0.06	11.11	0.99
			1,270.8	0.0085	0.68	0.15	0.00	7.69	0.90			1,307.6	0.027	8.13	0.87	0.03	11.11	0.98
	Cu	4	63.5	0.0014	0.21	0.01	2.92	0.08	0.86	Zn	4	65.3	0.012	0.55	0.86	0.002	-1.38	0.90

			158.5	0.0008	0.83	0.86	1.55	0.10	0.93			163.4	0.014	0.49	0.84	0.01	0.90	0.95	
			317.7	0.021	2.40	0.93	0.27	3.23	0.99			327	0.023	2.09	0.71	0.14	3.57	0.99	
			635.4	0.0074	3.16	0.93	0.0007	6.67	0.92			653.8	0.024	4.57	0.95	0.02	4.55	0.91	
			1,270.8	0.026	10.47	0.94	0.007	12.5	0.86			1,307.6	0.027	11.48	0.91	0.003	10.00	0.90	
				0.011	1.41	0.46	0.008	2.44	0.99				0.004	0.99	0.12	0.09	0.8	0.89	
BC350	Cu	6	63.5							Zn	6	65.3							
			158.5	0.018	1.48	0.55	0.16	2.56	0.98			163.4	0.012	1.48	0.91	0.15	1.64	0.98	
			317.7	0.018	2.40	0.58	0.36	5.26	0.99			327	0.016	1.20	0.73	0.07	1.49	0.91	
			635.4	0.017	3.47	0.49	0.48	8.33	0.99			653.8	0.013	2.63	0.63	0.15	4	0.99	
			1,270.8	0.0039	2.40	0.03	0.06	8.33	0.99			1,307.6	0.026	6.17	0.87	0.05	9.09	0.99	
	Cu	5	63.5	0.017	0.32	0.42	0.34	0.54	0.91	Zn	5	65.3	0.015	0.25	0.96	0.37	0.25	0.93	
			158.5	0.018	0.83	0.65	0.12	1.18	0.89			163.4	0.008	1.58	0.91	0.005	2.33	0.92	
			317.7	0.02	1.38	0.75	0.23	2.17	0.99			327	0.005	3.55	0.90	0.06	2.22	0.94	
			635.4	0.01	1.62	0.25	0.87	3.23	0.99			653.8	0.025	5.89	0.90	0.07	8.33	0.99	
			1,270.8	0.017	5.25	0.68	0.01	3.45	0.82			1,307.6	0.032	13.49	0.95	0.006	12.5	0.85	
	Cu	4	63.5	0.01	0.50	0.95	0.01	0.78	0.87	Zn	4	65.3	0.01	0.20	0.77	0.01	0.47	0.90	
			158.5	0.01	0.16	0.96	0.77	0.14	0.87			163.4	0.013	0.30	0.82	0.07	0.37	0.91	
			317.7	0.01	2.57	0.83	0.11	2.78	0.98			327	0.033	2.82	0.98	0.09	3.13	0.98	
			635.4	0.008	1.32	0.95	0.06	0.97	0.91			653.8	0.025	2.82	0.99	0.06	3.13	0.96	
			1,270.8	0.023	7.59	0.98	0.01	8.33	0.88			1,307.6	0.011	0.79	0.73	0.001	12.5	0.94	

1

2 Continued

AC Norit	Cu	6	63.5	0.032	0.52	0.65	1.93	1.69	0.99	Zn	6	65.3	0.012	0.45	
				0.08	0.23	1.15	0.95						0.06	4.17	0.91
			163.4	0.016	4.07	0.93	0.02	4.55	0.74	158.5	0.012	3.80	0.83	0.06	4.17
			327	0.012	2.51	0.95	0.003	4.17	0.78	317.7	0.014	3.24	0.77	4.00	5
			635.4	0.021	2.34	0.99				653.8	0.0073	1.95	0.11	0.07	5.88
			1,270.8	0.011	6.92	0.42	2.13	12.5	0.98	1,307.6	0.018	6.31	0.71	3E-05	50
	Cu	5	63.5	0.0043	0.68	0.15	0.76	0.50	0.92	Zn	5	65.3	0.011	0.25	
			163.4	0.02	1.62	0.30	0.17	0.84	0.91	158.5	0.013	2.82	0.71	0.09	1.14
			327	0.022	2.40	0.62	0.09	2.38	0.95	317.7	0.02	2.24	0.84	1.14	2.70
			635.4	0.026	4.37	0.75	0.09	5.56	0.99	653.8	0.021	4.68	0.68	0.09	9.09
			1,270.8	0.026	9.55	0.94	0.005	10	0.86	1,307.6	0.013	16.98	0.43	0.004	16.67
	Cu	4	63.5	0.023	0.69	0.55	0.07	0.45	0.76	Zn	4	65.3	0.015	0.32	0.13
			163.4	0.023	0.74	0.0042	0.39	0.09	0.47	317.7	0.023	6.61	0.85	0.02	5.88
			327	0.021	5.50	0.90	0.02	5.26	0.88	635.4	0.015	3.24	0.015	3.24	0.63
			635.4	0.028	6.61	0.69	0.008			1,270.8	0.011	12.5	0.94		
			1,270.8	0.0079	5.89	0.26	0.49	7.14	0.94	1,307.6	0.0093	9.33	0.23	2.45	14.29

AC Fluval	Cu	6	63.5	0.02	1.26	0.80	2.01	1.35	0.99	Zn	6	65.3	0.0035	0.11
			158.5	0.0089	2.29	0.67	1.69	2.56	0.97	163.4	0.021	3.16	0.85	0.40
			317.7	0.021	3.16	0.85	0.40	4.76	0.99	635.4	0.025	5.37	0.82	0.25
			635.4	0.017	4.37	0.93	0.11	5.56	0.98	1,270.8	0.023	9.09	0.99	0.99
			1,270.8	0.017	12.5	0.99				1,307.6	0.021	5.37	0.66	0.07
	Cu	5	63.5	0.0078	0.71	0.37	8.25	0.50	0.95	Zn	5	65.3	0.013	0.47
			163.4	0.011	1.66	0.93	0.17	1.45	0.91	158.5	0.011	1.29	0.36	0.81
			317.7	0.014	1.45	0.82	0.02	1.47	0.89	327	0.014	1.86	0.66	0.11
			635.4	0.014	1.86	0.66	0.11	2.33	0.97	653.8	0.038	5.37	0.92	0.92

0.08	4.55	0.98			653.8	0.03	8.51	0.99	0.03	10	0.97			1,270.8
0.035	8.91	0.88	0.02	3.57	0.87			1,307.6	0.021	5.25	0.95	0.10	7.14	0.99
Cu	4	63.5	0.01	0.11	0.60	6.21	0.02	0.82	Zn	4	65.3	0.005	0.24	0.04
1.49	0.11	0.68			158.5	0.0097	0.32	0.20	1.46	0.10	0.91			163.4
0.005	0.59	0.24	1.23	0.29	0.81			317.7	0.021	1.82	0.44	0.15	3.33	0.99
		327	0.028	3.55	0.70	0.06	3.57	0.96			635.4	0.015	1.23	0.47
0.10	1.19	0.84			653.8	0.023	3.89	0.76	0.002	6.67	0.77			1,270.8
0.013	3.16	0.53	0.17	6.67	0.98			1,307.6	0.02	3.24	0.40	0.16	14.29	0.99
Biomass Cu	6	63.5	0.0063	0.84	0.48	1.15	0.77	0.87	Zn	6	65.3	0.0062	0.15	0.50
4.66	0.11	0.96			158.5	0.018	1.95	0.70	0.11	0.8	0.92			163.4
									0.012	0.81	0.39	13.2	0.92	0.96
317.7	0.017	2.57	0.96	0.05	1.30	0.85	327	0.0066	0.85	0.22	0.19	1.06	0.83	635.4
0.64	1,270.8	0.023	4.57	0.98	0.08	3.13	0.98	1,307.6	0.014	2.00	0.41	0.05	4.35	0.95
Cu	5	63.5	0.016	0.50	0.53	1.24	0.60	0.99	Zn	5	65.3	0.012	0.49	0.21
0.49	0.69	0.95			158.5	0.018	1.35	0.62	0.25	1.25	0.95			163.4
0.018	0.90	0.37	0.26	1.01	0.94			317.7	0.027	2.75	0.88	0.07	2.04	0.90
								327	0.0005	0.32	0.40	0.60	1.35	0.99
635.4	0.01	1.58	0.22	0.07	3.70	0.97	653.8	0.015	2.34	0.51	0.06	3.57	0.95	1,270.8
5.88	0.76							1,270.8	0.023	3.24	0.95	0.11	3.23	0.98
1,307.6	0.025	4.68	0.74	0.008										
Cu	4	63.5	0.013	1.00	0.66	0.36	0.50	0.93	Zn	4	65.3	0.0022	0.22	0.31
1.24	0.26	0.91			158.5	0.02	0.81	0.36	0.31	1.89	0.95			163.4
0.0004	0.18	0.20	0.39	0.49	0.90			317.7	0.017	1.22	0.49	0.10	2.33	0.92
		327	0.0027	0.26	0.01	0.41	0.93	0.95			635.4	0.0078	1.01	0.07
0.04	4.35	0.80			653.8	0.0058	0.46	0.05	0.28	1.27	0.99			1,270.8
0.012	1.66	0.32	0.03	5.26	0.85			1,307.6	0.012	1.32	0.35	0.06	1.92	0.83

1

- 2 According to the results, the correlation coefficients obtained by the pseudo-second-order
- 3 kinetic model as well as qq_{ee} were higher than those of the pseudo-first-order kinetic model
- 4 ($R^2 < 0.90$), suggesting that the entire adsorption process was better described by a kinetic of a 5
- 5 second-order. The goodness of the pseudo-second-order kinetic towards the experimental 6
- 6 results was further confirmed by the smaller confidence intervals (with few exceptions for tests
- 7 at pH 4) obtained between $Q_e(\text{exp})$ and $Q_e(\text{cal})$ (Table S1), suggesting that the chemisorption

1 process favored by covalent or valency forces, and sharing of electrons may be the rate-limiting
2 step (Ho and Mckay, 1999).

3

4 **3.2.2 Adsorption isotherms**

5 Langmuir and Freundlich estimated model parameters for all adsorbents investigated are given
6 in Table 4. According to the obtained correlation coefficient (R^2) for copper, Langmuir model
7 fitted the experimental data better than Freundlich for the substrates investigated at different
8 pH values (higher average R^2 value nearly 0.90), confirming a strong copper-biochar's surface
9 interaction. Moreover, Freundlich parameter ($1/n$) for copper adsorbed at pH 5 and 6 was below
10 one, confirming a Langmuir-type isotherm. On the other hand, as also observed by others
11 (Sheet et al., 2014), zinc showed a better correlation coefficient, $1/n$ and k parameter for
12 Freundlich isotherm, indicating that each metal possesses different mechanisms of adsorption.

13 **Table 4.** Langmuir and Freundlich Isotherms parameters for Cu and Zn adsorption onto
14 BC600ACT, BC350ACT, BC600 and BC350 at different pHs.

Adsorbent	Model	Parameters	Cu			Zn		
			pH4	pH5	pH6	pH4	pH5	pH6
BC600ACT	Langmuir	Q_{max}	5.91	0.36	14.28	1.41	14	3.33
		K	0.002	0.006	0.004	0.006	0.0006	0.006
		R^2	0.94	0.88	0.93	0.98	0.57	0.88
BC600ACT	Freundlich	K_f	0.07	1.92	2.02	0.05	0.93	0.25
		$1/n$	2.20	0.65	0.62	1.81	0.57	1.19
		R^2	0.70	0.82	0.96	0.96	0.59	0.91
BC350ACT	Langmuir	Q_{max}	6.17	8.87	19.72	2.88	23.58	7.38
		K	0.002	0.006	0.004	0.003	0.0005	0.006
		R_2	0.89	0.97	0.96	0.75	0.36	0.98
BC350ACT	Freundlich	K_f	1.05	2.18	2.56	1.01	1.03	1.26
		$1/n$	0.56	0.43	0.65	0.30	0.75	0.72
		R_2	0.86	0.84	0.97	0.26	0.85	0.97
BC600	Langmuir	Q_{max}	7.69	7.19	14.51	2.02	22.22	11
		K	0.002	0.003	0.005	0.008	0.0005	0.002
		R_2	0.20	0.88	0.98	0.93	0.73	0.89
BC600	Freundlich	K_f	0.02	1.45	1.88	0.05	1.07	0.19
		$1/n$	1.91	0.43	0.77	1.91	0.76	1.48
		R_2	0.85	0.63	0.98	0.96	0.78	0.93
BC350	Langmuir	Q_{max}	0.71	2.98	13.21	1.85	5.31	9.34
		K	0.005	0.006	0.003	0.003	0.002	0.002
		R_2	0.94	0.94	0.94	0.88	0.93	0.85
BC350	Freundlich	K_f	0.08	1.16	2.08	0.03	0.73	0.44
		$1/n$	2.21	0.19	0.52	2.06	0.85	0.93
		R_2	0.78	0.13	0.90	0.96	0.85	0.94
AC norit	Langmuir	Q_{max}	2.85	12.34	13.36	5.34	6.75	5.15
		K	0.011	0.01	0.038	0.001	0.017	0.033
		R_2	0.97	0.99	0.96	0.94	0.86	0.98
AC norit	Freundlich	K_f	0.14	0.87	2.38	0.03	0.76	1.90
		$1/n$	1.326	0.70	0.57	2.05	0.92	0.39

		R₂	0.63	0.95	0.92	0.89	0.66	0.56
AC fluval	Langmuir	Q_{max}	1.66	6.06	17.54	2.64	8.29	14.7
		K	0.017	0.017	0.022	0.0006	0.01	0.009
		R₂	0.99	0.98	0.84	0.79	0.76	0.31
AC fluval	Freundlich	K_f	0.14	1.06	1.74	0.043	1.10	0.34
		1/n	1.22	0.53	0.66	1.92	0.67	1.11
		R₂	0.71	0.91	0.93	0.94	0.69	0.95

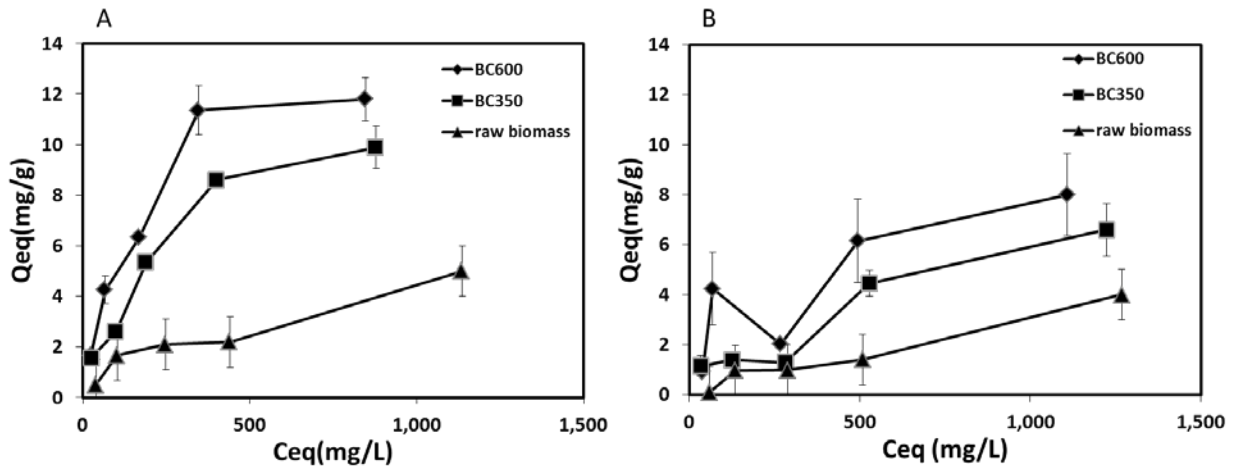
1

2

15 **3.2.3 Effect of pyrolysis temperature**

16 The adsorption of copper and zinc at pH 6 by raw *Miscanthus x giganteus* biomass, BC
17 pyrolyzed at 350 and 600°C is shown in Figure 4. Experimental results showed a higher
18 removal capacity of BC600 respect to BC350 and raw biomass. Statistical analysis revealed a
19 significantly higher capacity of copper removal by BC600 compared to BC350, while for zinc
20 this difference was statistically reported to be non-significant. Similar tendencies were also
21 observed for both metals (Cu and Zn) at pH 4 and pH 5 (data not shown).

22



23

24

25 **Figure 4.** Uptake capacity of metals by BC600, BC350 and raw biomass for Cu (A) and Zn (B),
26 respectively at pH6.

27

28 Figure 4 shows the impact of pyrolysis temperature on the removal capacity of biochar. This
29 trend is in line with the results illustrated in Table 1, which showed a higher pore size of
30 BC600 respect to BC350. As observed by others (Kim et al., (2012), during pyrolysis, the
31 possible loss of volatile matter fosters the removal of functional groups elements (H, O and N),
32 the atomic ratio reduces, amorphous carbon increase and microstructure develops (Table 1 and
33 2). These characteristics can favor adsorption processes by which van der Waals forces are
34 involved, while for BC350 cation exchange might be favored, due to the presence of carboxyl
35 functional groups. These results are in accordance with the elemental analysis results (Table 1)

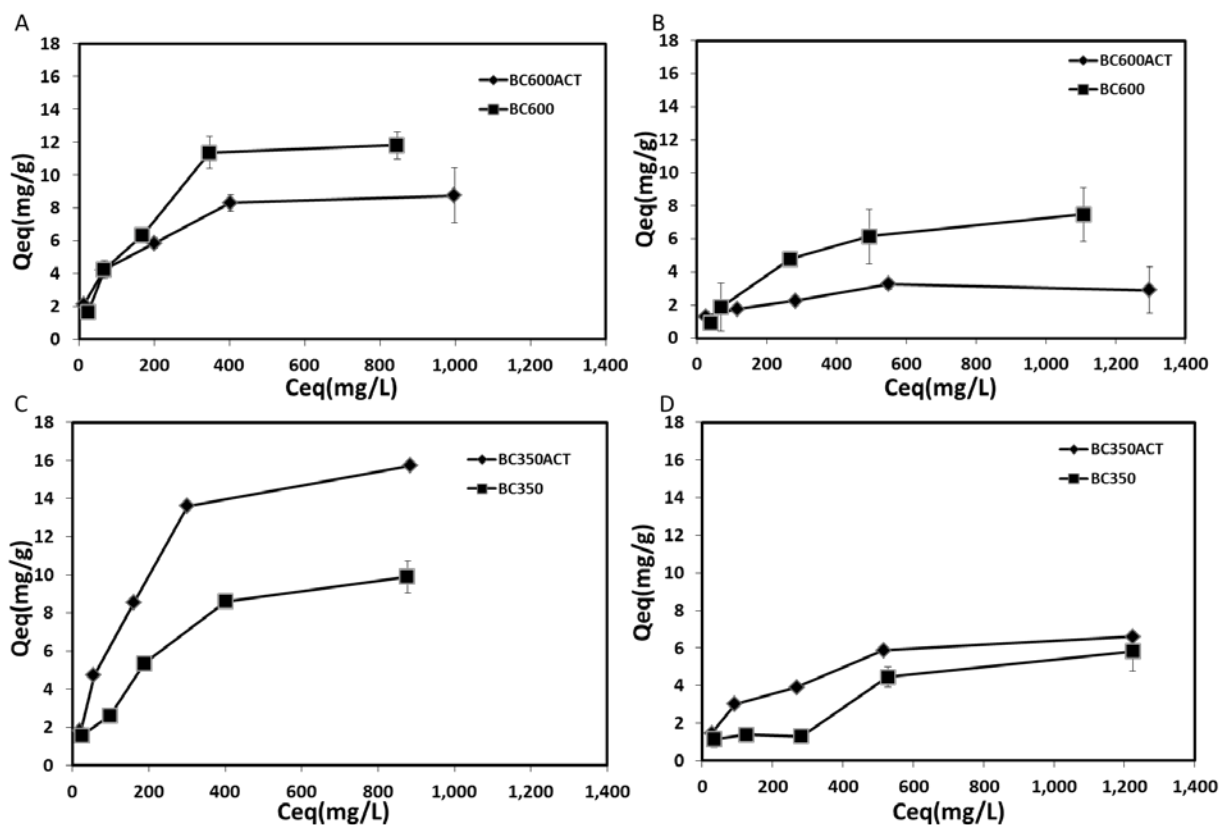
36 and FTIR results (Table 2), which showed a decrease of H, O and N elements with consequent
37 reduction of functional groups and the shift to an aromatic structure. Moreover, the
38 predominant aromatic structure of BC600 provides π -electron density, which is known to bond
39 metal cation to carbon, resulting in the formation of organometallic compounds (Harvey et al.,
40 2011). Similarly, other researchers (Kolodynska et al., 2012), showed that biochars produced
41 at high pyrolysis temperature had higher metal adsorption capacities.

42

43 ***3.2.4 Effect of chemical activation by H₂O₂***

44 The chemical modification was investigated by using hydrogen peroxide. As a matter of fact,
45 being H₂O₂ a strong oxidizing agent ($E_{\text{O}_{\text{H}_2\text{O}_2/\text{H}_2\text{O}} = 1.78 \text{ V}$) it could provide enough oxidizing
46 power to transform hydroxyl and aldehyde groups into carboxylic ones, thereby enhancing the
47 coordination capability and, eventually, the sorption capacity. As illustrated in Figure 5, the
48 chemical activation by H₂O₂ showed two main results: BC600ACT did not show any enhanced
49 adsorption capacity respect to BC600, while BC350ACT showed an enhanced removal
50 capacity respect to BC350. Despite substantiation that the chemical activation by H₂O₂ lead to
51 increase the oxygen-containing functional groups as indicated in Table 2 and metal-
52 complexing functional groups (Fig. 1), particularly carboxyl groups which enhance the metal
53 adsorption capacity (Xue et al., 2012), there are also examples that exhibit a lesser effect (Yin
54 et al., 2007).

55



56
57
58 **Figure 5.** Effect of H₂O₂ activation on BC600 and BC350 for Copper (A-C) and zinc (B-D) at
59 pH6.
60

61 The reduced adsorption capacity of BC600ACT respect to BC600 is given by a detrimental
62 effect of the chemical oxidation on the physical aspect of the biochar. Indeed, along with a
63 negligible change in BET surface area, BC600 ACT had a reduced pore size (Table 1) that may
64 be attributable to the destruction of porous structure and textural characteristic within BC due
65 to the severe oxidation (Yin et al., 2007). Moreover, due to an enhanced dehydration during
66 the pyrolysis, the biochar produced at 600°C had a lower content of electron-enriched
67 functional groups, thus resulting into a negligible chemical activation. Conversely, chemical
68 activation improved notably the physic-chemical characteristics of biochar pyrolyzed at lower
69 temperature, showing the highest BET surface area, highest oxygen content, highest O/C and
70 H/C ratios (Table 1 and 2), and increased intensity of the O-H stretching of the hydroxyl groups
71 at 3200-3400 cm⁻¹ (Fig. 1), reflecting in a higher adsorption capacity. The greater effect of

72 oxidation on biochar pyrolyzed at lower temperature could be due to the lower degree of fused
73 aromatic C structures (Kim et al., 2011). The correlation between effectiveness of H₂O₂
74 treatment and biochar pyrolysis temperature was also observed by Xue et al. (2012) and Wang
75 et al. (2016) which, respectively reported the positive effect of H₂O₂ modification on biochar
76 pyrolyzed at 300° C and a non-relevant effect of H₂O₂ activation on biochar pyrolyzed at 600°
77 C in terms of cations removal capacity.

78

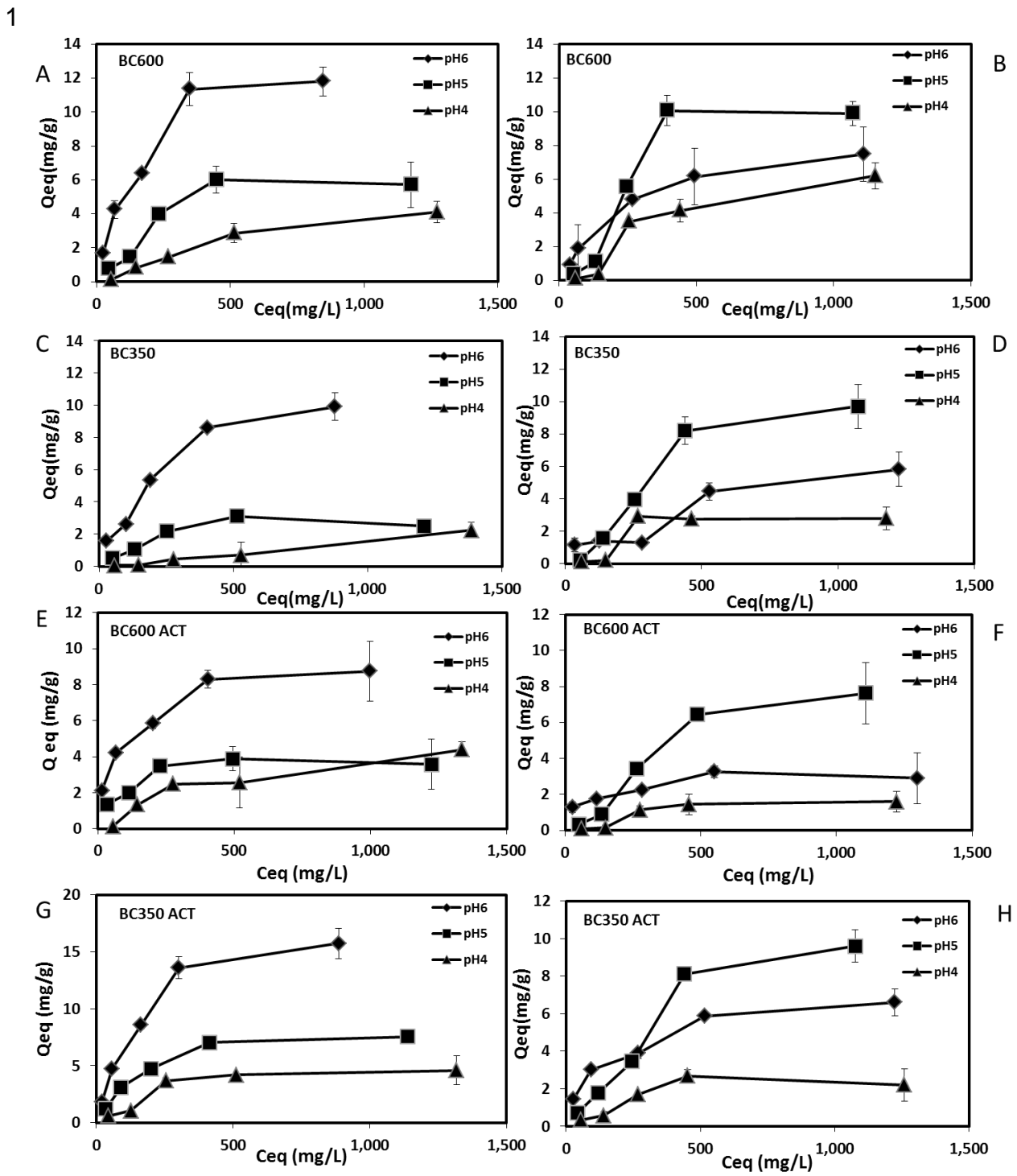
79 ***3.2.5 Effect of pH***

80 The effect of pH on the removal efficiency is shown in Figure 6. Given the higher hydrogen
81 ion competition at lower pH, both metals were adsorbed in larger extent at higher pH values.
82 Indeed, at higher pH values, the weakly acidic nature of the active sites (carboxyl groups) of
83 the biochar, favors the deprotonation process and increases the negative charge of biochar's
84 surface, facilitating the metals cations uptake (Kolodynska et al., 2012)). Similar studies have
85 observed an increase of metals' uptake with increasing the pH up to five, claiming as main
86 factor the competition between protons and metal cations for surface sorption sites on the
87 biochars (Chen et al., 2011; Liu and Zhang, 2009; Mohan et al., 2007). Moreover, the metals'
88 uptake increased with the metals' concentration probably due to the fact that low copper and
89 zinc concentrations were not enough to consume the alkali ions released by biochar's surface.

90

91

92



2
 3 **Figure 6.** Effect of pH value on the adsorption capacity of Miscanthus biochar: BC600 (A
 4 and B for Cu and Zn, respectively); BC350 (C and D for Cu and Zn, respectively); BC600ACT
 5 (E and F for Cu and Zn, respectively); BC350ACT (G and H for Cu and Zn, respectively).
 6

7 Under the pH range investigated in this study (4-6), maximum copper removal was at pH 6,
 8 while zinc at pH 5. As reported by Harvey et al. (2011), heavy metals are predominately

9 adsorbed via electrostatic interactions, while other mechanisms such as ion exchange and $C\pi$ -

1 metal bonding by basic carbon are less favoured. At higher pH, electrostatic interactions are
 2 favoured by active sites deprotonated, facilitating copper uptake (Mc Bride, 1994; Fontes et
 3 al., 2000). However, despite the pH was kept under control during the experiments, it cannot
 4 be excluded the formation of copper (hydr)oxide precipitation which may hinder the interaction
 5 between zinc cations and biochar's active site (Li et al., 2013). All biochars investigated
 6 showed a preferential adsorption of copper at pH 6 while zinc at pH 5 (Figure 6). Among the
 7 biochars investigated, the highest adsorption amount was obtained by BC350 ACT for copper
 8 (15.7 mg/g), however for all biochars used copper showed a stronger affinity respect to zinc,
 9 as well as demonstrated by other studies (Chen et al., 2011; Seco et al., 1997;). Importantly,
 10 biochars' adsorption capacities were comparable with AC fluval and AC norit (activated
 11 carbons) tested in parallel in this study (Table 5), and with other biochars reported in literature,
 12 such as animal manure biochar, hardwood biochars and corn-straw derived biochar (between 5
 13 to 6 mg/g, 12.51 and 6.79 mg/g, respectively) (Kolodynska et al., 2012; Chen et al., 2011),
 14 confirming the effectiveness of *Miscanthus x giganteous* derived biochar to remove copper and
 15 zinc.

16 **Table 5.** Copper and zinc adsorption (mg/g) for biomass, BC350ACT, BC600ACT, BC350
 17 and BC600, AC Fluval and AC Norit GAC. Results show averages \pm standard error (n=2).

Adsorbent	Cu (mg/g)			Zn (mg/g)		
	pH 4	pH 5	pH 6	pH 4	pH 5	pH 6
BC600 ACT	4.3 \pm 0.4	3.8 \pm 0.6	8.7 \pm 1.6	2.6 \pm 0.5	7.6 \pm 1.6	3.2 \pm 0.3
BC350 ACT	4.6 \pm 1.2	7.9 \pm 0.4	15.7 \pm 1.3	3.3 \pm 0.3	9.6 \pm 0.8	6.6 \pm 0.7
BC600	4.1 \pm 0.6	6.3 \pm 0.7	11.8 \pm 0.8	7.3 \pm 0.7	10.4 \pm 0.8	8 \pm 1.6
BC350	3 \pm 0.4	3.1 \pm 0.4	9.9 \pm 0.8	2.9 \pm 0.1	9.7 \pm 1.3	5.8 \pm 1
AC Norit	6.6 \pm 2.3	6.3 \pm 0.9	11.3 \pm 1.6	6.6 \pm 1	17.9 \pm 2.9	5 \pm 0.6
AC Fluval	5.5 \pm 0.9	4.7 \pm 0.1	11.1 \pm 0.7	3.2 \pm 0.6	8.8 \pm 0.2	7.2 \pm 1.1
Biomass	1.67 \pm 0.7	2.2 \pm 0.2	5 \pm 0.8	1.83 \pm 0.3	3.2 \pm 0.4	4 \pm 0.6

18
 19 Given the pH-dependent metals' uptake mechanisms involved for copper and zinc removal, a
 20 study about the determination of the distribution coefficient (K_d) and the selectivity coefficient
 21 (α) was conducted. As summarized in Table 6, the α values (α_1) observed at pH 6 were at least

22 3 times higher than those observed at pH 4 and 5, indicating a preferential adsorption of copper
 23 to zinc at pH 6 for all biochars investigated. Conversely, according to the α_2 values, zinc
 24 showed adsorption selectivity to copper at pH 5.

25 The preferential adsorption of copper to zinc could be explained by the capacity of copper to
 26 form covalent bonds, and this ability can be related to ionization potential and ionic radius
 27 (softness of a metal), as derived by Misono et al. (1967). Other researchers (Basta and
 28 Tabatabai, 1992), reported that copper was preferentially adsorbed to zinc by soil on the basis
 29 of softness parameter. McBride (1994), also explained the higher affinity and preferential
 30 retention of metals by other parameters like electronegativity and ionic radii. However,
 31 AbdElfaltah and Wada (1981), found that the metal retention could not be predicted only from
 32 electronegativity and ionic radii. These controversial results suggests that the metal retention
 33 affinity might involve both covalent and electrostatic bonds. Therefore, it can be concluded
 34 that the higher affinity of copper respect to zinc for surface complexation and electrostatic
 35 reactions can be explained by higher electronegativity (copper= 2.0; zinc= 1.6), larger softness
 36 value (2.89 for copper and 2.34 for zinc) and hydrolysis constant (7.3-8.0 for copper and 9.09.4
 37 for zinc) (Abd-Elfaltah and Wada 1981; Basta and Tabatabai, 1992; Misono et al., 1967;
 38 Shaheen et al., 2012)).

39
 40
 41
 42

	4	9.21	20.35	0.45	2.20
BC600ACT	5	0.65	14.44	0.04	22.9

	6	41.87	25.09	1.66	0.59
	4	9.61	22.53	0.43	2.32
Adsorbent	pH	K_d -Cu (L/g)	K_d -Zn (L/g)	α^1	α^2
Table 6. Competitive binding behaviors of BC600ACT, BC350ACT, BC600 and BC350 for Cu ²⁺ (aq), and Zn ²⁺ (aq) ions. α_1 : Selectivity of copper over zinc. α_2 : Selectivity of zinc over copper.					
BC350 ACT	5	8.26	17.84	0.46	2.16
	6	50.27	21.51	2.34	0.43
BC600	4	15.31	31.86	0.48	2.08
	5	9.41	18.50	0.51	1.97
	6	55.71	35.60	1.56	0.64
BC350	4	10.05	26.49	0.38	2.64
	5	1.82	18.06	0.10	9.93
	6	44.44	15.31	2.90	0.34

4. Conclusions

This study demonstrated that *Miscanthus x giganteus* derived biochars effectively remove copper and zinc from synthetic wastewater. The temperature of pyrolysis plays an important role on the physic-chemical structure of biochar, affecting the metal removal capacity. Biochar pyrolyzed at higher temperature showed an enhanced metal removal capacity for both copper and zinc. The activation of biochar by H₂O₂ resulted to be pyrolysis-temperature sensitive, leading to enhanced metals removal capacity of the biochar pyrolyzed at lower temperature (BC350 ACT) for both copper and zinc. The effect of pH revealed that zinc was predominantly removed at pH 5 while copper at pH 6, opening new interesting scenarios about the possible selective removal and recovery of these two metals by *Miscanthus x giganteus* derived biochar. Biochars' metals removal capacities resulted to be comparable with commercially available activated carbons. Overall *Miscanthus x giganteus* derived biochar could be a valid alternative to activated carbon for an efficient removal of metal ions.

61

62 **Acknowledgements**

63 This study was supported by an International Fellowship funded by the University of Rome
64 “La Sapienza” and by the Short Term Scientific Mission (CSCM) within the COST scientific
65 programme on Biochar as an option for sustainable resource management. The authors would
66 like to acknowledge the School of Chemistry and Physics of University of KwaZulu-Natal
67 (Westville campus) for FT-IR, BET and elemental analysis.

68 **References**

- 69 Abd-Elfaltah, A., Wada. K., 1981. “Adsorption of lead, copper, zinc, cobalt and cadmium by
70 soils that differ in cation exchange materials. *Soil Sci.* 32, 271– 283.
- 71 Al-Wabel, M.I., Al-Omran, A., El-Naggar, A.H., Nadeem, M., Usman, A.R.A., 2013. Pyrolysis
72 temperature induced changes in characteristics and chemical composition of biochar produced
73 from conocarpus wastes. *Bioresour. Technol.* 131, 374–379. Akbal, F., Camci, S., 2011.
74 Copper, chromium and nickel removal from metal plating wastewater by
75 electrocoagulation. *Desalination* 269 (1–3), 214–222.
- 76 Basta, N.T., Tabatabai, M.A., 1992. Effect of cropping systems on adsorption of metals by
77 soils. III. Competitive adsorption. *Soil Sci.* 153, 331-337.
- 78 Bradl, H. B., 2004. Adsorption of heavy metal ions on soils and soils constituents. *J. Colloid*
79 *Interface Sci.* 277, 1–18.
- 80 Brosse, N., Dufour, A., Meng, X., Sun, Q., Ragauskas, A., 2012. Miscanthus: a fast-growing
81 crop for biofuels and chemicals production. *Biofuel Bioprod. Bior.* 6(5), 580-98.
- 82 Brunauer, S., Emmett, P.H., Teller, E., 1938. Adsorption of Gases in Multimolecular Layers.
83 *J. Am. Chem. Soc.* 60 (2), 309–319.

84 Boudrahem, F., Soualah, A., Aissani-Benissad, F., 2011. Pb(II) and Cd(II) removal from
85 aqueous solutions using activated carbon developed from coffee residue activated with
86 phosphoric acid and zinc chloride. *J. Chem. Eng. Data.* 56 (5), 1946–1955.

87 Bouwman, R., Freriks, I.L.C., 1980. Low-temperature oxidation of a bituminous coal. Infrared
88 spectroscopic study of samples from a coal pile. *Fuel.* 59 (5), 315-322.

89 Cao, X., Harris, W., 2010. Properties of dairy-manure-derived biochar pertinent to its potential
90 use in remediation. *Bioresour. Technol.* 101, 5222–5228.

91 Chen, X.C., Chen, G.C., Chen, L.G., Chen, Y.X., Lehmann, J., McBride, M.B, Hay, A.G.,
92 2011. Adsorption of copper and zinc by biochars produced from pyrolysis of hardwood
93 and corn straw in aqueous solution. *Bioresour Technol.* 102, 8877–8884.

94 Cheng, C.H., Lehmann, J., Engelhard, M.H., 2008. Natural oxidation of black carbon in soils:
95 Changes in molecular form and surface charge along a climosequence. *Geochimica et*
96 *Cosmochimica Acta.* 72, 1598–1610.

97 Clifton-Brown, J.C., Breuer, J., Jones, M.B., 2007. Carbon mitigation by the energy crop,
98 *Miscanthus*. *Glob Change Biol.* 13(11), 2296-307.

99 Dabrowski, A., Hubicki, Z., Podkoscielny, P., Robens, E., 2004. Selective removal of the heavy
100 metal ions from waters and industrial wastewaters by ion-exchange method.
101 *Chemosphere.* 56, 91-106.

102 EPA, 2016. Secondary Drinking Water Standards: Guidance for Nuisance Chemicals.
103 [https://www.epa.gov/dwstandardsregulations/secondary-drinking-water-](https://www.epa.gov/dwstandardsregulations/secondary-drinking-water-standardsguidance-nuisance-chemicals)
104 [standardsguidance-nuisance-chemicals](https://www.epa.gov/dwstandardsregulations/secondary-drinking-water-standardsguidance-nuisance-chemicals)

105 Fontes, M.P.F. Matos, A.T., Costa, L.M., Neves, J.C.L., 2000. Competitive adsorption of zinc,
106 cadmium, copper and lead in three highly-weathered Brazilian soils. *Commun. Soil Sci.*
107 *Plant Anal.* 31, 2939-2958.

108 Fontes, M.P.F., Gomes, P.C., 2003. Simultaneous competitive adsorption of heavy metals by
109 the mineral matrix of tropical soils. *Appl. Geochem.* 18, 795-804.

110 Fox, J., 2008. *Applied regression models and generalized linear models* (2nd ed.). Thousand
111 Oaks, CA: SAGE.

112 Fu, F., Xie, L., Tang, B., Wang, Q., Jiang, S., 2012. Application of a novel strategy-Advanced
113 Fenton-chemical precipitation to the treatment of strong stability chelated heavy metal
114 containing wastewater. *Chem. Eng. J.* 189–190, 283–287.

115 Gerente, C., Lee, V.K.C., Le Cloirec, P., McKay, G., 2007. Application of Chitosan for the
116 Removal of Metals from Wastewaters by Adsorption—Mechanisms and Models
117 Review. *Critical Reviews in Environ. Sci. and Technol.* 37, 41–127.

118 Gregorich, E.G., Carter, M.R., 1997. *Soil Quality for Crop Production and Ecosystem Health.*
119 *Developments in Soil Science.* 25, 1-448.

120 Harvey, O.R., Herbert, B.E., Rhue, R.D., Kuo, L.J., 2011. Metal interactions at the
121 biocharwater interface. Energetics and structure-sorption relationships elucidated by
122 flow adsorption microcalorimetry. *Environ. Sci. Technol.* 45 (13), 5550-5556.

123 Heaton, E., Long, S., Voigt, T., Jones, M., Clifton-Brown, J., 2004. *Miscanthus for renewable*
124 *Energy generation: European union experience and projections for illinois. Mitig Adapt*
125 *Strateg. Glob Change.* 9(4), 433-51.

126 Houben, D., Sonnet, P., Cornelis, J.T., 2014. Biochar from *Miscanthus*: a potential silicon
127 fertilizer. *Plant Soil.* 374:871–882.

128 Ho, Y.S., McKay, G., 1999. The kinetics of sorption of divalent metal ion onto *Sphagnum* moss
129 peat. *Water Res. J.* 34(3), 735-742.

130 Huff, M.D., Lee, J.W., 2016. Biochar-surface oxygenation with hydrogen peroxide. *J. Environ.*
131 *Manage.* 165, 17–21.

132

- 133 Kang, T., Park, Y., Yi, J., 2004. Highly Selective Adsorption of Pt^{2+} and Pd^{2+} Using
134 ThiolFunctionalized Mesoporous Silica. *Ind. Eng. Chem. Res.* 43, 1478-1484.
- 135 Kim, P., Johnson, A., Edmunds, C.W., Radosevich, M., Vogt, F., Rials, T.G., Labb'e, N., 2011.
136 Surface functionality and carbon structures in lignocellulosic-derived biochars
137 produced by fast pyrolysis. *Energy Fuels.* 25, 4693–4703.
- 138 Kołodyńska, D., Wnętrzak, R., Leahy, J.J., Hayes, M.H.B., Kwapiński, W., Hubicki, Z.,
139 2012. Kinetic and adsorptive characterization of biochar in metal ions removal. *Chem*
140 *Eng J.* 197, 295–305.
- 141 Kim, H. K., Kim, J.-Y., Cho, T.S., Choi, J.W., 2012. Influence of pyrolysis temperature on
142 physicochemical properties of biochar obtained from the fast pyrolysis of pitch pine
143 (*Pinus rigida*). *Bioresour. Technol.* 118, 158–162.
- 144 Kwapinski, W., Byrne, C.M.P., Kryachko, E., Wolfram, P., Adley, C., Leahy, J.J., et al., 2010.
145 Biochar from biomass and waste. *Waste Biomass Valor.* 1(2), 177-89.
- 146 Lagergren, S., 1898. About the theory of so-called adsorption of soluble substances.
147 *Kungl. Sv. Vetenskapsakad. Handlingar.* 24, 1.
- 148 Li, N., Bai, R.B., Liu, C.K., 2005. Enhanced, selective adsorption of mercury ions on chitosan
149 beads grafted with polyacrylamide via surface-initiated atom transfer radical
150 polymerization. *Langmuir.* 21, 11780–11787.
- 151 Li, M., Liu, Q., Guo, L.J., Zhang, Y.P., Lou, Z.J., Wang, Y., Qian, G.R., 2013. Cu(II) removal
152 from aqueous solution by *Spartina alterniflora* derived biochar. *Bioresour. Technol.*
153 141, 83–88.
- 154 Lim, A.P., Aris, A.Z., 2013. A review on economically adsorbents on heavy metals removal in
155 water and wastewater. *Environ. Sci. Biotechnol.* 13, 163-181.
- 156 Lin, Y. H., Fryxell, G. E., Wu, H., Engelhard, M., 2001. Selective Sorption of Cesium Using
157 Self-Assembled Monolayers on Mesoporous Supports. *Environ. Sci. Technol.* 34,
158 3962-3966.

159 Liu, Z., and Zhang, F.S., 2009. Removal of lead from water using biochars prepared from
160 hydrothermal liquefaction of biomass. *J. Hazard. Mater.* 167, 933–939.

161 Lewandowski, I., Clifton-Brown, J., Scurlock, J., Huisman, W., 2000. Miscanthus: European
162 experience with a novel energy crop. *Biomass Bioenergy.* 19(4), 209-27.

163 Malamis, S., Katsou, E., Haralambous, K.J., 2011. Study of Ni(II), Cu(II), Pb(II), and Zn(II)
164 removal using sludge and minerals followed by MF/UF. *Water Air Soil Pollut.* 218(14),
165 81-92.

166 Margui, E., Salvado, V., Queralt, I., Hidalgo M., 2004. Comparison of three-stage sequential
167 extraction and toxicity characteristic leaching tests to evaluate metal mobility in mining
168 wastes. *Anal. Chem. Acta.* 524, 151–159.

169 McBride, M.B., 1994. *Environmental Chemistry of Soils.* Oxford University Press, New York,
170 NY, USA.

171 Melligan, F., Dussan, K., Auccaise, R., Novotny, E.H., Leahy, J.J., Hayes, M.H.B., 2012.
172 Characterisation of the products from pyrolysis of residues after acid hydrolysis of
173 Miscanthus. *Bioresour. Technol.* 108, 258-63.

174 Meng, J., Feng, X., Dai, Z., Liu, X., Wu, J., Xu, J., 2014. Adsorption characteristics of Cu(II)
175 from aqueous solution onto biochar derived from swine manure. *Environ. Sci. Pollut.*
176 *Res.* 21, 7035–7046.

177 Mimmo, T., Panzacchi, P., Baratieri, M., Davies, C.A., Tonon, G., 2014. Effect of pyrolysis
178 temperature on miscanthus (*Miscanthus x giganteus*) biochar physical, chemical and
179 functional properties. *Biomass and bioenergy.* 62, 149-157.

180 Misono, M., Ochiai, E., Saito, Y., Yoneda, Y., 1967. A new dual parameter scale for the
181 strength of Lewis acids and bases with the evaluation of their softness. *J. Inorg. Nucl.*
182 *Chem.* 29, 2685-2691.

183 Mohan, D., Pittman, C.U., Bricka, M., Smith, F., Yancey, B., Mohammad, J., Steele, P.H.,
184 Alexandre-Franco, M.F., Gomez-Serrano, V., Gong, H., 2007. Sorption of arsenic,
185 cadmium, and lead by chars produced from fast pyrolysis of wood and bark during
186 biooil production. *J. Colloid. Interface Sci.* 310, 57–73.

187 Moreira, C.S., Alleoni, L.R. F., 2010. Adsorption of Cd, Cu, Ni and Zn in tropical soils under
188 competitive and non-competitive systems. *Sci. Agric. (Piracicaba, Braz.)*. 67, 301-307.

189 Novak, J.M., Lima, I., Xing, B., Gaskin, J.W., Steiner, C., Das, K.C., Ahmedna, M.A., Rehrh,
190 D., Watts, D.W., Busscher, W.J., Schomberg, H., 2009. Characterization of designer
191 biochar produced at different temperatures and their effects on a loamy sand. *Ann.*
192 *Environ. Sci.* 3, 195–206.

193 Seco, A., Marzal, P., Gabaldón, C., Ferrer, J., 1997. Adsorption of heavy metals from aqueous
194 solutions onto activated carbon in single Cu and Ni systems and in binary Cu–Ni, Cu–
195 Cd and Cu–Zn systems. *J. Chem. Technol. Biotechnol.* 68, 23– 30.

196 Shaheen, S.M., Derbalah, A.S., Moghanm, F.S., 2012. Removal of Heavy Metals from
197 Aqueous Solution by Zeolite in Competitive Sorption System. *International Journal of*
198 *Environ. Sci. Deve.* 3 (4), 362-367..

199 Sheet, I., Kabbani, A., Holail, H., 2014. Removal of Heavy Metals Using Nanostructured
200 Graphite Oxide, Silica Nanoparticles and Silica/ Graphite Oxide. *Composite Energy*
201 *Procedia.* 50, 130 – 138.

202 Sun, R.C., Tomkinson, J., 2001. Fractional separation and physico-chemical analysis of lignins
203 from the blackliquor of oil palm trunk fibre pulping. *Sep. Purif. Technol.* 24(3),
204 529539.

205 Tchounwou, P., Yedjou, C.G., patlolla, A.K., Sutton, D.J., 2012. Heavy metals toxicity and the
206 environment. *EXS.* 101, 133-164.

207 Trevino-Cordero, H., Juárez-Aguilar, L.G., Mendoza-Castillo, D.I., Hernández-Montoya, V.,
208 Bonilla-Petriciolet, A., Montes-Morán, M.A., 2013. Synthesis and adsorption
209 properties of activated carbons from biomass of *Prunus domestica* and *Jacaranda*
210 *mimosifolia* for the removal of heavy metals and dyes from water. *Ind. Crops Prod.* 42,
211 315–323.

212 Turan, N.G., Elevli, S., Mesci, B., 2011. Adsorption of copper and zinc ions on illite:
213 Determination of the optimal conditions by the statistical design of experiments. *Appl.*
214 *Clay Sci.* 52, 392–399.

215 Wang, S.H., Griffiths, P.R., 1985. Resolution enhancement of diffuse reflectance Ir-spectra of
216 coals by fourier self-deconvolution: 1. C-H stretching and bending modes. *Fuel.* 64,
217 229–236.

218 Wang, X.J., Liang, X., Wang, Y., Wang, X., Liu, M., Yin, D.Q., Xia, S.Q., Zhao, J.F., Zhang,
219 Y.L., 2011. Adsorption of copper (II) onto activated carbons from sewage sludge by
220 microwave-induced phosphoric acid and zinc chloride activation. *Desalination.* 278,
221 231–237.

222 Wang, B., Lehmann, J., Hanley, K., Hestrin, R., Enders, A., 2016. Ammonium retention by
223 oxidized biochars produced at different pyrolysis temperatures and residence times.
224 *RSC Adv.* 6, 41907-41913.

225 Xue, Y., Gao, B., Yao, Y., Inyang, M., Zhang, M., Zimmerman, A. R., Ro, K.S., 2012.
226 Hydrogen peroxide modification enhances the ability of biochar (hydrochar) produced
227 from hydrothermal carbonization of peanut hull to remove aqueous heavy metals: Batch
228 and column tests. *Chem. Eng. J.* 200–202, 673–680.

229 Yao, Y., Gao, B., Inyang, M., Zimmerman, A.R., Cao, X., Pullammanappallil, P., Yang, L.,
230 2011. Removal of phosphate from aqueous solution by biochar derived from
231 anaerobically digested sugar beet tailings. *J. Hazard. Mat.* 190, 501–507.

- 232 Yin, C.Y., Aroua, M. K., Wan Daud, W. M. A., 2007. Review of modifications of activated
233 carbon for enhancing contaminant uptakes from aqueous solutions. *Sep. Purif. Technol.*
234 52, 403–415.
- 235 Yuan, J., Xu, R., Zhang, H., 2011. The forms of alkalis in the biochar produced from crop
236 residues at different temperatures. *Bioresour. Technol.* 102, 3488–3497.